



## Nature and Evolution of the Fusion Boundary in Ferritic-Austenitic Dissimilar Weld Metals, Part 1 — Nucleation and Growth

*A model for heterogeneous nucleation along the fusion boundary is proposed*

BY T. W. NELSON, J. C. LIPPOLD AND M. J. MILLS

**ABSTRACT.** A fundamental investigation of fusion boundary microstructure evolution in dissimilar-metal welds (DMWs) between ferritic base metals and a face-centered-cubic (FCC) filler metal was conducted. The objective of the work presented here was to characterize the nature and character of the elevated-temperature fusion boundary to determine the nucleation and growth characteristics of DMWs. Type 409 ferritic stainless steel and 1080 pearlitic steel were utilized as base metal substrates, and Monel (70Ni-30Cu) was used as the filler metal. The Type 409 base metal provided a fully ferritic or body-centered-cubic (BCC) substrate at elevated temperatures and exhibited no on-cooling phase transformations to mask or disguise the original character of the fusion boundary. The 1080 pearlitic steel was selected because it is austenitic at the solidus temperature, providing an austenite substrate at the fusion boundary. The weld microstructure generated with each of the base metals in combination with Monel was fully austenitic.

In the Type 409/Monel system, there was no evidence of epitaxial nucleation and growth as normally observed in ho-

mogenous weld metal combinations. The fusion boundary in this system exhibited random grain boundary misorientations between the heat-affected zone (HAZ) and weld metal grains. In the 1080/Monel system, evidence of normal epitaxial growth was observed at the fusion boundary, where solidification and HAZ grain boundaries converged. The fusion boundary morphologies are a result of the crystal structure present along the fusion boundary during the initial stages of solidification. Based on the results of this investigation, a model for heterogeneous nucleation along the fusion boundary is proposed when the base and weld metals exhibit ferritic (BCC) and FCC crystal structures, respectively.

### Introduction

The importance of joining and cladding of dissimilar metals has increased substantially in all aspects of manufacturing over the past two decades. Applications of dissimilar-metal welds (DMWs) include cladding for corrosion resistance and joining base metals that exhibit large differences in structure and properties, *i.e.*, plain carbon or low-alloy steels to austenitic stainless steels. This trend can be expected to continue with the increasing use of duplex and super-austenitic stainless steels. Cracking associated with DMWs has been a persistent problem, resulting in significant economic loss over the past several decades. Cracking in DMWs typically occurs near the fusion boundary either along the martensitic transition immediately adjacent to the fusion boundary or along the Type II boundary in the weld metal. This Type II boundary parallels the fusion boundary typically less than 100  $\mu\text{m}$  away in the weld metal.

The evolution, nature and role of weld metal interfaces in promoting or mitigating weld-related cracking are not well understood. The implications of boundaries and structures with regards to crack growth rates, fatigue, stress corrosion cracking, etc., have been researched extensively in the materials science arena. In spite of the recurring problems and economic losses, the role of boundaries

### KEY WORDS

Dissimilar-Metal Welds  
Epitaxial Growth  
Fusion Boundary  
HAZ  
Microstructure  
Monel  
Pearlitic Steel

*T. W. NELSON, formerly with The Ohio State University, is now with Brigham Young University, Provo, Utah. J. C. LIPPOLD and M. J. MILLS are with The Ohio State University, Columbus, Ohio.*







sis. Standard metallographic techniques were used to prepare optical and SEM samples. Because of the different characteristics of the base and weld metal, two etchants were used for metallographic preparation of samples. These included the following: 1) 4% nital, which etches the pearlitic steel; and 2) an electrolytic solution of 5 g Fe<sub>3</sub>Cl, 2 mL of HCL and 99 mL of methanol for the weld metal. Optical microscopy and scanning electron microscopy (SEM) were used for microstructure characterization of structures and boundaries along the fusion boundary. Optical metallography was performed at magnifications up to 400X and SEM up to 1600X.

**Electron Microscopy Analysis**

Electron backscatter diffraction analyses were performed on both TEM thin foils and bulk metallographically prepared samples. Samples were loaded in the SEM at an angle of 70 deg from the incident beam toward a phosphor detector. The electron beam was then rastered across the sample in a hexagonal grid at specified increments. Kikuchi signals were automatically analyzed using OIM™ software (Refs. 12–14). This software calculates the Euler angles of the electron backscatter diffraction (EBSD) patterns with reference to the sample normal, then stores the position and angles of each pattern. These data were then used for various grain boundary and texture analysis.

**Results**

**Optical Microscopy**

The resulting microstructures produced in the Type 409/Monel system are shown in Figs. 3 and 4. Over the range of BMDs investigated, all welds exhibited roughly the same microstructures along the fusion boundary. In general, the HAZ exhibited a large, fully ferritic grain structure typical of fully ferritic materials with insufficient secondary phases present to hinder grain growth. The weld metal exhibited a fully FCC cellular or cellular/dendritic microstructure with no evidence of epitaxial growth observed at any of the BMDs produced. This is very evident in Fig. 4, where the HAZ and SGBs at the fusion boundary are not continuous; instead, they intersect the fusion boundary at roughly mid-grain of one another. In homogeneous metal welds, the HAZ grain boundary and SGB would be continuous across the fusion boundary, and the misorientation across these boundaries would be the same.

Another interesting microstructural

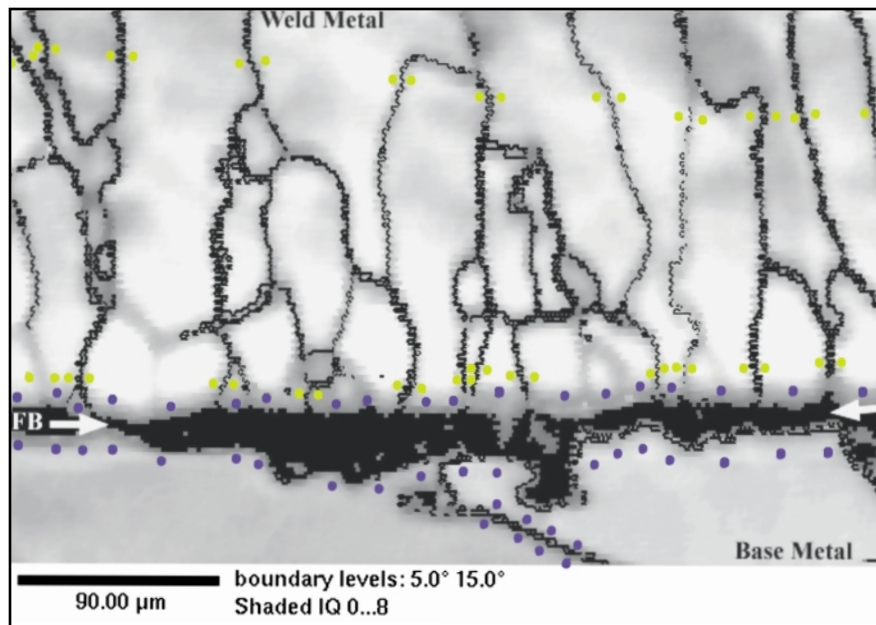


Fig. 6 — Image quality grain map of fusion boundary region in Type 409/Monel base and filler metal.

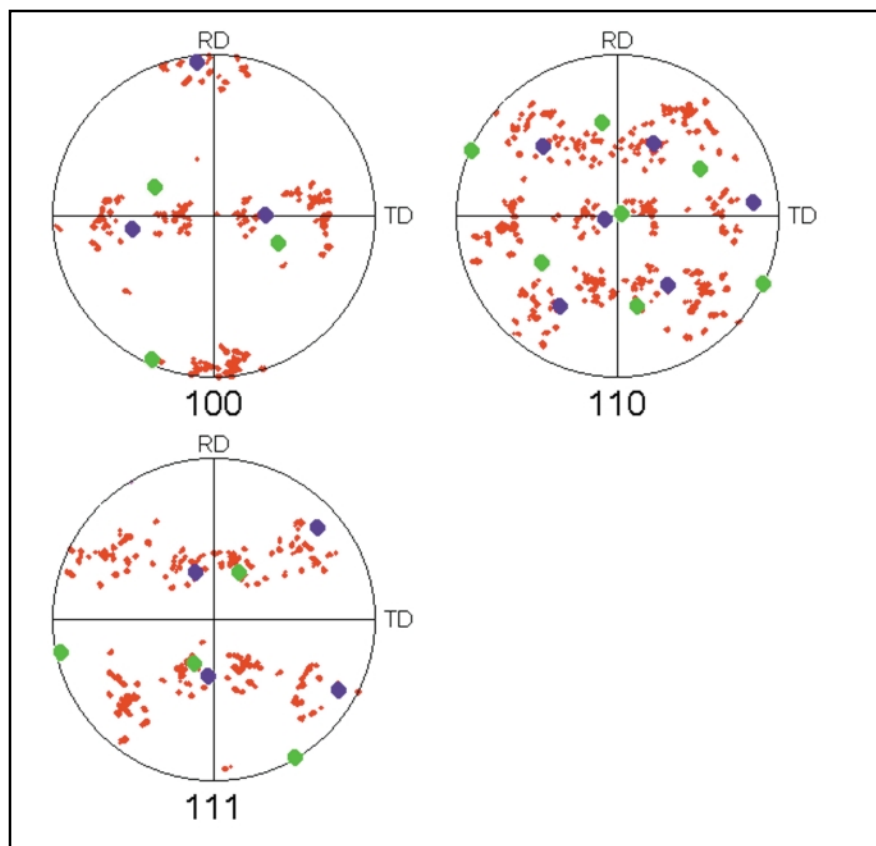


Fig. 7 — Discrete pole figures showing individual orientations by color from grain map shown in Fig. 6. Base metal grains are represented by the large blue and green spots while the weld metal grains are represented by small red spots.







boundary junctions, interfacial steps or discontinuities, secondary phases, etc. Because these nuclei form at heterogeneous sites on the HAZ interface, they may or may not exhibit those preferred orientation relationships observed in FCC/BCC systems. As a result, the fusion boundary is likely to exhibit random misorientations between base and weld metal grains.

It was the intent of the present investigation to gain a better understanding of the nature and evolution of the fusion boundary during the initial stages of solidification in DMWs. From this basis, it is possible to postulate the theories and mechanisms that explain the nature and evolution of those boundaries and their susceptibility to failure in DMWs in engineering applications, such as pressure vessel steels clad with austenitic stainless steels. A subsequent paper will explain the nature and evolution of the fusion boundary during the cooling portion of the weld thermal cycle and the effects of the  $\delta$ - $\gamma$  and  $\gamma$ - $\alpha$  transformations. Likewise, the nature and evolution of the Type II boundary and its susceptibility to cracking will be explained.

## Conclusions

1) The effect of base metal and weld metal microstructure at elevated temperature significantly influences the nature and evolution of the fusion boundary microstructure in dissimilar metal welds.

2) When the base and weld metal exhibit different crystal structures (BCC/FCC) at the solidification temperature, nucleation of solid weld metal occurs on heterogeneous sites on the partially melted HAZ grain at the fusion boundary.

3) When different crystal structures are present, the fusion boundary exhibits

random misorientations between base and weld metal grains as a result of heterogeneous nucleation in the weld pool. The various misorientations along the fusion boundary may or may not exhibit some of those preferred BCC/FCC relationships, *i.e.*, Bain, Kurdjumov-Sachs, and Nishiyama-Wasserman.

4) When the base and weld metal exhibit the same crystal structure at the solidus temperature, standard weld metal epitaxial growth may occur despite significant differences in composition.

5) Although the fusion boundary does not exhibit the typical cube-on-cube relationship, weld solidification proceeds in the normal  $\langle 100 \rangle$  easy growth direction.

## Acknowledgments

This work was supported by Dr. John C. Lippold at The Ohio State University. The authors wish to thank INCO Alloys for providing the filler metal used in this investigation. Technical support provided by the Welding and Joining Metallurgy Group at The Ohio State University was greatly appreciated.

## References

1. Shewmon, P. G. 1983. *Transformations in Metals*. Jenks, Okla.: J. Williams Book Co.
2. Chalmers, B. 1967. *Principles of Solidification*. New York, N.Y.: John Wiley & Sons, Inc.
3. Flemings, M. C. 1974. *Solidification Processing*. New York, N.Y.: McGraw-Hill Publishing Co.
4. Kou, S. 1987. *Welding Metallurgy*. New York, N.Y.: John Wiley & Sons, Wiley Interscience.
5. Savage, W. F. 1980. Solidification, segregation and weld imperfections. *Welding in the World* 18(5-6): 89-114.
6. Savage, W. F., and Hrubec, W. J. 1972. Synthesis of weld solidification using crystalline organic materials. *Welding Journal* 51(5): 260-s to 271-s.

7. Savage, W. F., Lundin, C. D., and Aronson, A. H. 1965. Weld metal solidification mechanisms. *Welding Journal* 44(4):175-s to 181-s.

8. Savage, W. F., and Aronson, A. H. 1966. Preferred orientation in the weld fusion zone. *Welding Journal* 45(2):85-s to 89-s.

9. Samuel, J. 1979. Crystallography in fusion-weld-metal solidification mechanics. Ph.D. diss. Rensselaer Polytechnic Institute, Troy, N.Y.

10. Lippold, J. C., Clark, W. A. T., and Tumuluru, M. 1992. An investigation of weld metal interfaces. *The Materials Science of Joining*. Edited by M. J. Cieslak, J. H. Perepezlo, and M. E. Glicksman, The Minerals, Metals & Materials Society, pp. 141-145.

11. Porter, D. A., and Easterling, K. E. 1981. *Phase Transformations in Metals and Alloys*. Berkshire, England: Van Nostrand Reinhold International.

12. Adams, B. L. 1993. Orientation imaging microscopy: Application to the measurement of grain boundary structure. *Materials Science and Engineering A166*: 59-66.

13. Wright, S. I. 1993. A review of automated orientation imaging microscopy (OIM). *Journal of Computer-Assisted Microscopy* 5(3):207-221.

14. Adams, B. L., Wright, S. I., and Karsten, K. 1993. Orientation imaging: The emergence of a new microscopy. *Met. Trans. A* 24A: 819-831.

15. Jackson, K. A., Hunt, J. D., Uhlmann, D. R., and Seward, T.P., III. 1966. On the origin of the equiaxed zone in castings. *Trans. AIME* 236(2):149-158.

16. Bower, T. F., and Flemings, M. C. 1967. Structure of dendrites at chill surfaces. *Trans. AIME* 239:1620-1625.

17. Hellawell, A., and Herbert, P. M. 1962. Proceeding of the Royal Society, A269.

18. Savage, W. F., Nippes, E. F., and Erickson, J. S. 1976. Solidification mechanisms in fusion welds. *Welding Journal* 55(8):213-s to 221-s.

19. Davies, G. J., and Garland, J. G. 1975. Solidification structures and properties of fusion welds. *International Metallurgical Reviews* 20:83-106.

## REPRINTS REPRINTS

To Order Custom Reprints of  
Articles in the

*Welding Journal*

Call Denis Mulligan  
at (800) 259-0470

## REPRINTS REPRINTS